

A New Method for Wide Frequency Range Dynamic Olfactory Stimulation and Characterization

Andrew S. French and Shannon Meisner

Department of Physiology and Biophysics, Dalhousie University, Halifax,
Nova Scotia B3H1X5, Canada

Correspondence to be sent to: Andrew S. French, Department of Physiology and Biophysics, Dalhousie University, Halifax, Nova Scotia B3H1X5, Canada. e-mail: andrew.french@dal.ca

Abstract

Sensory receptors often receive strongly dynamic, or time varying, inputs in their natural environments. Characterizing their dynamic properties requires control and measurement of the stimulus over a frequency range that equals or exceeds the receptor response. Techniques for dynamic stimulation of olfactory receptors have lagged behind other major sensory modalities because of difficulties in controlling and measuring the concentration of odorants at the receptor. We present a new method for delivering olfactory stimulation that gives linear, low-noise, wide frequency range control of odorant concentration. A servo-controlled moving bead of silicone elastomer occludes the tip of a Pasteur pipette that releases odorant plus tracer gas into a flow tube. Tracer gas serves as a surrogate indicator of odorant concentration and is measured by a photoionization detector. The system has well-defined time-dependent behavior (frequency response and impulse response functions) and gives predictable control of odorant over a significant volume surrounding the animal. The frequency range of the system is about 0–100 Hz. System characterization was based on random (white noise) stimulation, which allows more rapid and accurate estimation of dynamic behavior than deterministic signals such as sinusoids or step functions. Frequency response functions of *Drosophila* electroantennograms stimulated by fruit odors were used to demonstrate a typical application of the system.

Key words: antenna, *Drosophila*, frequency response, impulse response, olfaction, photoionization, sensory receptor

Introduction

The dynamic properties of a wide range of electrical, mechanical, and biological systems have traditionally been measured by linear systems analysis. An example is to stimulate a photoreceptor, with a series of sinusoidal oscillations in light intensity at different frequencies while measuring the resulting sinusoidal membrane potential fluctuations. Calculating the gain (ratio of output amplitude to input amplitude) and phase (shift of the wave in time) at each frequency then gives the frequency response function. Importantly, it can be shown that if the system behaves linearly, the frequency response function can be used to predict the response of the system to any other stimulus, and it, therefore, provides a complete dynamic description of the system (Bendat and Piersol 1980).

Sinusoidal stimulation is only one method of characterizing a linear system. Other methods use step functions and other deterministic or predictable signals. An important concept is the impulse response function, which is the response of the system to an (theoretical) impulse that is infinitely narrow and infinitely high but has unit area. The impulse response can be calculated from other stimulation methods

and is widely used to represent the dynamic properties of systems.

Although sinusoids and other deterministic signals are important theoretically, modern systems analysis often uses a random unpredictable signal, commonly called “white noise.” A random signal can be represented by the sum of many different sinusoids with randomly distributed amplitudes and phases, allowing the system to be rapidly characterized over a wide frequency range by a brief measurement of its response to the noise. White noise stimulation has become a standard approach for characterizing linear, and some cases nonlinear, biological systems (French et al. 1972; Marmarelis PZ and Marmarelis VZ 1978).

Dynamic properties of sensory receptors are crucially important for understanding the ranges of external stimuli that animals can detect, as well as the types and quantities of information transmitted to central nervous systems. Dynamic characterization can also place quantitative limits on the physiological components that could be responsible for sensory transduction and sensory information coding (Marmarelis PZ and Marmarelis VZ 1978). Measuring the dynamic

response of a sensory structure requires accurate control of its input stimulus. This was achieved relatively early for some mechanoreceptors (Pringle and Wilson 1959) and for photoreceptors (Fuortes and Hodgkin 1969) and has been followed by detailed linear and nonlinear systems analysis of both types of receptors (French and Wong 1977; Marmarelis and Naka 1973).

Olfaction and gustation are important senses for both vertebrates and invertebrates and the activities of moth olfactory projection neurons have been shown to vary in response to dynamic stimulation (Vickers et al. 2001). However, characterizing dynamic responses of chemoreceptors has proved more difficult because of the nature of the stimulus. The basic requirements for linear and nonlinear systems analysis of sensory receptors are the abilities to modulate the signal in a controlled manner over a wide range of frequencies and to accurately measure both the input stimulus signal and the output neural signal with appropriate time resolution.

Dynamic stimulation of some insect olfactory receptors has been achieved using pulsed release of chemicals in wind tunnels (Bau et al. 2005). Another approach used randomly varying pheromone concentration produced by turbulent flow in a wind tunnel (Justus et al. 2005). There has also been progress in detecting rapidly changing airborne chemical concentration by photoionization of tracer gas with low-ionization potential added to the chemical stimulant (Justus et al. 2005; Vetter et al. 2006). Complete dynamic characterization of an unknown system ideally requires an input stimulus with a frequency range, or bandwidth, exceeding that of the system. Little evidence is available about the functional frequency ranges of olfactory systems, but moth electroantennograms responded to frequencies from zero to at least 50 Hz (Justus et al. 2005), so a stimulus range of 0–100 Hz is a reasonable initial target for characterization of insect olfactory receptors. It is also important for the input signal spectrum to be smooth (similar amplitude at all frequencies), so that the system response can be detected at most frequencies within the range. Currently available stimulation systems have limited dynamic control of odorant concentration and are highly dependent on physical design and construction (Vetter et al. 2006). This reduces their ability to stimulate sensory receptors over their complete dynamic ranges.

Here, we describe a new dynamic odorant stimulation system that overcomes these major limitations by providing controlled, wide bandwidth olfactory stimulation to insects or other animals. *Drosophila* was used for initial system development because they have become an important model of olfaction with the discovery of many olfactory receptor genes and both anatomical and functional mapping of their distribution (Dobritsa et al. 2003; Vosshall et al. 1999). Many natural odors detected by *Drosophila* have been found (Stensmyr et al. 2003), and it is clear that odor receptors in the antenna vary in their dynamic properties as well as their relative chemical selectivities (Yao et al. 2005).

Design of the olfactory stimulation system evolved from a series of experiments based on previous work with larger insects in wind tunnels (Justus et al. 2005) and on pulsed stimulation of *Drosophila* antennae (Yao et al. 2005). The major design criterion was to deliver odorant with dynamically controlled and measured concentration to allow input–output systems analysis of olfactory receptor responses. A second important criterion was related to the difficulty of measuring tracer gas concentration at the exact location of a sensillum. To overcome this problem, we aimed to have laminar flow of odorant over the antenna to give the same concentration of tracer and odorant at reasonable distances from the antenna. Finally, we sought to maximize the available frequency range of concentration changes to allow characterization of a similarly wide range of dynamic sensory responses.

Materials and methods

Stimulation

The olfactory stimulation system was based on a small wind tunnel (Figure 1). Major airflow was produced by a 60 × 15 mm computer CPU cooling fan (Proten DFC601512M, Cooler Guys, Kirkland, WA) at one end of a 90-mm square plexiglas box. The fan (nominally 12 V DC) was driven by a variable DC power supply that gave useful airflow control in the range 4–12 V. Air flowed through a honeycomb of cut drinking straws (30 mm long × 5 mm diameter) to give laminar flow and then entered a circular plexiglas tube (22 mm internal diameter, 110 mm long). The fly was positioned at the far end of the tube, within 2–3 mm of the exit and 2–3 mm of the tube centerline.

Secondary airflow came from a cylinder of compressed air containing 1000 ppm propylene tracer gas (BOC, Halifax, NS, Canada), regulated to 20 kPa initial pressure. It flowed through an odorant cartridge made from the shaft of a 5-ml transfer pipette (Fisher Scientific, Ottawa, ON, Canada), containing a rectangular piece of filter paper (45 × 15 mm), into a Pasteur pipette whose tip was located in the center of the circular tube and 10 mm from one end. The tip of the pipette was variably occluded by a bead of silicone elastomer (Mastercraft tub and tile silicone sealant, Canadian Tire Corporation, Toronto, ON, Canada). The silicone elastomer was formed to a cylinder of approximately 5 mm length, 5 mm diameter, allowed to cure for 24 h and then one end was sliced to a flat surface with a razor blade. Pushing the bead against the tip of the pipette reduced the flow of gas. Placement of the circular flow tube within a larger chamber was designed to produce approximately equal air pressure on each side of the holes in the sides of the tube required for entry of the Pasteur pipette and silicone bead and reduce the possibility of producing turbulent flow.

Movement of the silicone bead against the pipette tip was controlled by a mechanical stimulator and sensed by

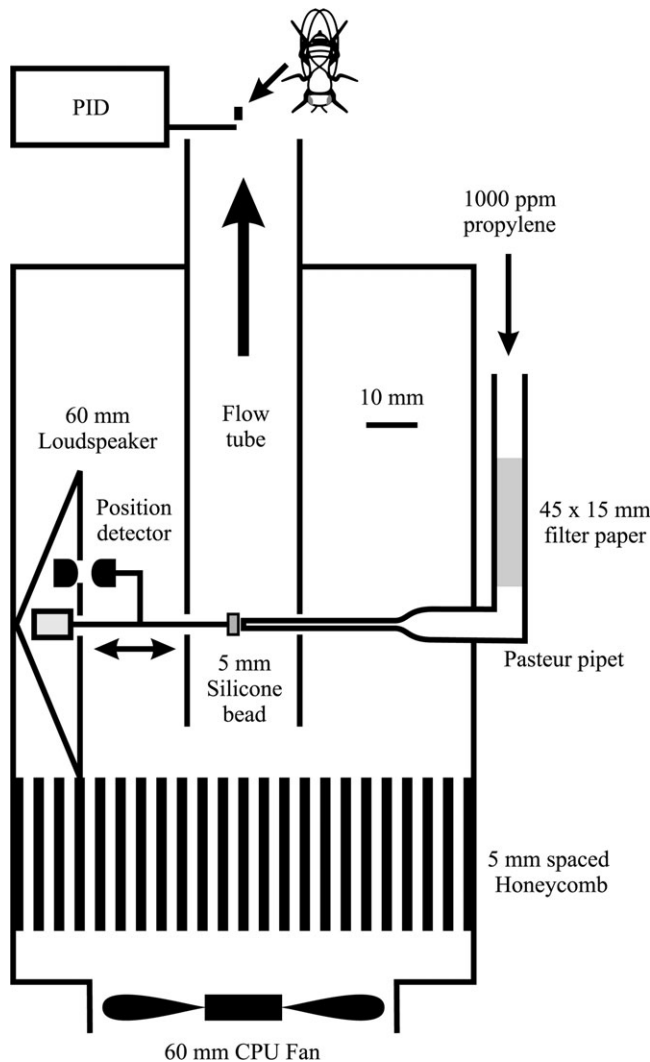


Figure 1 Plan view of the olfactory stimulation system. Major items are approximately to scale, excepting the PID. Experimental fly (*Drosophila*) is shown to approximate scale and also enlarged. Primary airflow was created by a 60-mm computer fan at the end of a 90-mm square plexiglas box. Laminar flow was induced by a honeycomb of cut drinking straws (5 mm diameter). Air flowed out through a circular plexiglas tube 115 mm long and 22 mm internal diameter (the flow tube). This was the only path for air to leave the box. Odorant chemicals were introduced by air flowing over a rectangular piece of filter paper (45 × 15 mm) in a cartridge made from a 5-ml transfer pipette. The air source contained 1000 ppm propylene as a tracer gas. Air containing mixed odorant and propylene tracer flowed through the tip of a Pasteur pipette located in the center of the circular tube, and 20 mm from its origin, via a small hole in the side of the tube. The Pasteur pipette tip was variably occluded by the flat surface of a 5-mm silicone elastomer bead, moved by the voice coil of a 60-mm loudspeaker. The position of the bead was detected by the voltage from a fixed infrared phototransistor illuminated by a matched infrared light-emitting diode mounted on the rod driving the bead. The fly was positioned in the center of the circular tube and 3 mm from its mouth. Tracer propylene was detected by a PID, with the mouth of the aspirating needle (0.76 mm internal diameter) located about 1 mm above the fly. Placement of the flow tube within a larger, fan-driven structure was designed to produce approximately equal air pressures inside and outside the tube at the locations where holes were necessary to admit the Pasteur pipette and the occluding bead and so reduce the possibility of turbulence at the stimulation site.

a position detector. Details of the position control system have been described previously (French and Kuster 1981; Widmer et al. 2006). Briefly, motion was produced by the voice coil of a 60-mm diameter loudspeaker (40-262 Radio Shack, Fort Worth, TX), whereas position was detected by a fixed infrared phototransistor illuminated by a matched infrared light-emitting diode on the shaft connected to the loudspeaker (276-142 Radio Shack 915 nm infrared pair). The position signal also provided second-order servo feedback control to the voice coil, with feedback loop compensation based on the open-loop properties of the system, including the weight of the silicone bead.

Odorant delivery

Odorant concentration and cartridge design were based on the stimulation system of Yao et al. (2005) for *Drosophila* antenna. In the present system, air carrying odorant was diluted about 1:100 by the main airflow, rather than about 1:1 for Yao et al., and the airflow rate over the odorant filter paper here was about twice as great (9 vs. 5 ml/s). To offset these dilution effects, we increased the odorant concentration from 1% to 20% and increased the filter paper area by about 5-fold (675 vs. 126 mm²), giving an overall estimated odorant delivery of about 50% compared with Yao et al. (2005). The actual odorant concentration depends on the evaporation rate from the filter paper, which is unknown and probably different for each odorant.

Four different odorants were used to test the system: butyl butyrate, isoamyl acetate, hexyl acetate, and phenylethyl alcohol. These are all naturally occurring fruit odorants that excite a range of *Drosophila* antennal olfactory receptors (Stensmyr et al. 2003). Odorant experiments were conducted using continuous flow of the main airstream before and after activating the secondary airflow containing the tracer gas and odorant. Odorant chemicals and mineral oil were purchased from Sigma (Oakville, ON, Canada) and mixed at 20% v/v. Fifty microliters of volumes of each mixture were loaded into separate cartridges. Fresh cartridges were prepared for each experiment.

Stimulus measurements

Experiments to characterize airflow through the stimulator used signals from the infrared position detector described above. The position detector was calibrated using a stereomicroscope containing an eyepiece graticule to observe movements of the flat surface of the silicone elastomer bead.

Tracer gas concentration was measured by a miniature photoionization detector (mini-PID, Model 200A, Aurora Scientific Inc., Aurora, ON, Canada). The PID samples the gas through an inlet needle probe. The tip of the probe was located directly above and within 1 mm of the fly antenna. The PID has a frequency response of 0–330 Hz and a concentration range of 0.05–500 ppm propylene. The typical

measurement range used here was 1–20 ppm. The PID inlet needle is 57 mm long with an internal diameter of 0.76 mm, giving a volume of 0.0259 cc. We used the lowest pump speed of 660 cc/min to minimize disturbance of airflow near the fly, giving a time delay of 2.35 ms. Additional delay must occur as the gas passes through the ionizing chamber, so we assumed a total delay of 3 ms. No detectable PID signal was seen in response to any of the odorants alone.

Electrophysiological measurements

Flies, *Drosophila melanogaster*, Oregon R #2376 (Bloomington *Drosophila* stock center, Bloomington, IN) were maintained in the laboratory. Flies of either sex were used within 2 days of hatching. Procedures for recording electroantennograms were similar to those described previously (Alcorta 1991). Animals were held in the cut end of a 100- μ l plastic pipette tip. A reference glass microelectrode electrode (\sim 1 μ m tip diameter) was inserted into one eye, whereas a larger glass microelectrode (\sim 20 μ m tip diameter) was pushed against the distal tip of one antenna. Both electrodes were filled with *Drosophila* saline (Hazel et al. 2003). Electroantennograms were recorded as electrical current with a List EPC-7 patch clamp amplifier (ALA Scientific Instruments, Westbury, NY). All experiments were performed at room temperature (20 ± 2 °C) in air at ambient humidity ($>50\%$).

Drosophila antennae are sensitive to sound and vibration, as well as chemicals. The experimental arrangement mechanically isolated the stimulation system from the preparation and recording electrodes by suspending the stimulation system on a separate mechanical mounting to the air-driven table holding the preparation. Sound insulation was also used around parts of the mechanical stimulator. Control experiments with no odorant chemicals gave no detectable responses. We also conducted control experiments with only the tracer gas present and again saw no significant responses.

Experimental control and data processing

All experiments were controlled by custom-written software via a personal computer and a data acquisition board (NI6035E, National Instruments, Austin, TX). Pseudorandom Gaussian white noise was generated by the computer via a 33-bit binary sequence algorithm driving a 12-bit digital-to-analog convertor into the position servo control. The position signal, PID voltage, and electroantennogram current were digitized via a 16-bit analog-to-digital convertor and sampled at 5-ms intervals. Sampled time domain data (20 000 input–output pairs) were transferred to the frequency domain using the fast Fourier transform (Cooley and Tukey 1965) in segments of 512 sample pairs. Frequency response functions between position signal (input) and PID voltage (output) or between PID voltage (input) and electroantennogram current (output) were calculated by direct

spectral estimation and plotted as Bode plots of phase and log gain versus log frequency. Gain may be conceptually viewed as the ratio of output over input amplitudes during sinusoid stimulation at a given frequency. Phase is the relative shift in time of the sinusoid between input and output, with 360° corresponding to a complete cycle of the sinusoid. Frequency response functions were fitted by a coherence-weighted minimum square error process.

The coherence function is a normalized measure of linear correlation between the input and output signals (Bendat and Piersol 1980). A value of unity indicates that all the output signal at a given frequency can be produced by a linear transformation of the input at that frequency. Values below unity mean either that some uncorrelated signal (noise) was added between the input and output or that the system behaved at least partially nonlinearly. Coherence functions were calculated from the same data as the frequency response functions.

The impulse response of a system is its theoretical response to an infinitely brief impulse input (a Dirac delta function). The impulse response is commonly used to represent the dynamic behavior of a system in the time domain, whereas the frequency response function provides the same information in the frequency domain. The frequency response and impulse functions can be mutually transformed to each other via the Fourier transform (Marmarelis PZ and Marmarelis VZ 1998). Impulse response functions were calculated from the same data, using the parallel cascade method (French and Marmarelis 1999).

Results

Dynamic control of odorant concentration

Characterization of the system was carried out using pseudorandom wide bandwidth (white noise) stimuli. This approach allows rapid, quantitative estimation of system dynamics and can be used to predict the system response to deterministic stimuli, such as pulses or sinusoids. Frequency response functions between silicone bead position and propylene trace gas concentration showed a linear, low-noise relationship with high coherence over the frequency range required for characterization of dynamic olfactory responses from *Drosophila* electroantennograms (Figure 2).

Approximate characterization of the fluid dynamics operating in the flow tube is possible by considering the theoretical response of the system to a brief impulse of air containing tracer gas and odorant from the mouth of the Pasteur pipette (Figure 1). Assuming laminar flow, the impulse would be detected by the PID at the end of the flow tube after a delay, Δt given by the tube length divided by the flow velocity. During this flow time, the impulse of gases would diffuse away from its center of mass in 3 dimensions into the surrounding volume of air. Several other factors, including frictional drag at the tube wall and silicone bead

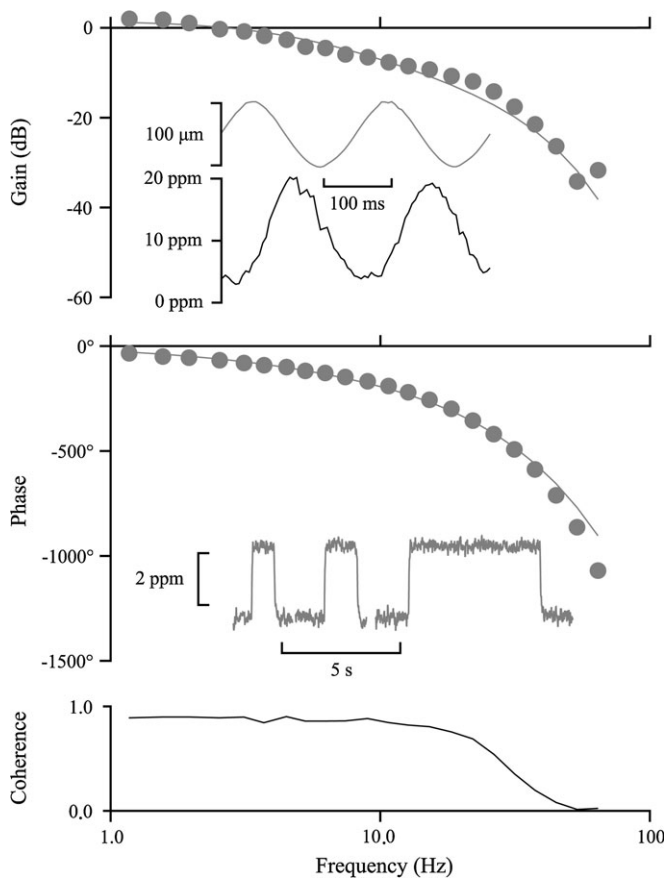


Figure 2 Frequency response of the odorant stimulation system, using random, wide bandwidth stimulation. Gain, phase, and coherence functions are shown between silicone bead position, sensed by the infrared phototransistor, and propylene tracer gas concentration detected by the PID at the mouth of the flow tube. Note the high coherence function over a broad frequency range, indicating an approximately linear, noise-free relationship between bead position and tracer concentration. Gain is shown in decibel units, with 0 db equivalent to 0.0236 ppm/ μm . Gain and phase data were fitted by equation (1), with the following parameters: $\alpha = 0.027$ ppm/ μm , $f_c = 47.4$ Hz, $\tau = 37.2$ ms, $\Delta t = 35.5$ ms. Upper inset shows original recordings of bead position (upper) and tracer concentration (lower) during sinusoidal stimulation at 5 Hz, illustrating sinusoidal modulation of gas concentration and the time delay due to airflow through the wind tunnel. Lower inset shows stimulation with small pulses of 1, 2, and 5 s duration. Note that these recordings are actual gas concentration measured at the animal.

would tend to delay and mix the gas, causing the amplitude of rapid concentration changes to be reduced relative to slow changes. We used a Gaussian function to model the diffusion effect and a first-order low-pass filter function to model the additional drag effects, giving the following frequency response function:

$$G(jf) = \alpha \cdot \exp(j\angle(2\pi f \Delta t)) \cdot \exp(-f/f_c)^2 \cdot 1/(1 + j2\pi f \tau), \quad (1)$$

where $G(jf)$ is the complex frequency response function (containing both gain and phase information), f is frequency,

and $j = \sqrt{-1}$. Parameter α is a constant amplitude factor with units of ppm propylene tracer per micrometer movement of the silicone bead (ppm/ μm). The second term in equation (1) is the phase lag due to the flow delay Δt , the third term is a Gaussian function with corner frequency f_c approximating diffusion, and the fourth term is a linear low-pass filter with time constant τ to approximate frictional drag. This equation was fitted to the gain and phase data in Figure 2 as solid lines.

Figure 2 also illustrates the ability of the system to deliver deterministic stimuli in the form of sinusoids and rectangular pulses. Note the accurate control, low-noise level, and ability to deliver constant concentration, even for small pulses. Also note that these traces represent actual concentration measured within about 1 mm of the animal, rather than at the upstream release site.

Temporal and spatial properties of the stimulus

The impulse response described above is the expected response to an input pulse that is infinitely high in amplitude, infinitely short in time, and has unit area. In this case, the area would be 1 ppm·s. Practical measurement of the impulse response is usually impossible because of the infinite amplitude, but it can be estimated for a linear system as the inverse Fourier transform of the frequency response function. It can also be estimated directly from the response of a system receiving white noise stimulation by the parallel cascade method, which has the advantage of removing any nonlinear components of the response (French and Marmarelis 1999). The impulse response provides an alternative view of system behavior and a more direct view of the time delay caused by flow along the tube. Impulse responses were estimated at the normal position of the PID probe, about 1 mm above the antenna, and then with the probe moved to a series of positions 5 mm away from the fly (Figure 3). The responses had the expected form of an approximately Gaussian distributed peak, delayed by about 44 ms from the release of tracer into the flow tube, combined with approximately exponential filtering that extended the response for at least 100 ms.

The close similarity between the impulse responses measured at different positions indicates that the dynamic tracer concentration was almost identical within a volume of at least 10 mm diameter surrounding the fly. Therefore, the PID signal can be expected to closely resemble the concentration of tracer, and hence odorant, at the antenna.

The mean time delay to the PID was 44 ms (Figure 3), but about 3-ms delay occurs within the PID probe (see Materials and Methods). The flow tube diameter was 2.2 cm, giving a cross-sectional area of 3.80 cm², and the distance from the Pasteur pipette tip to the fly was 9.7 cm, giving an effective volume of 36.9 cm³, a flow velocity 2.37 m/s and a volume flow of 899 cm³/s. The mean voltage from the PID during the experiments was held at approximately 1.7 V, corresponding to a concentration of 10 ppm propylene. Because the propylene concentration in the gas cylinder was 1000 ppm, the air

carrying the tracer gas, and odorant, was diluted about 1:100 by the system before reaching the fly.

Experimental test of the odorant stimulation system

Tests of the system used four different fruit odorants: butyl butyrate, isoamyl acetate, hexyl acetate, and phenylethyl alcohol. All the odorants produced clear positive responses (i.e., positive current increased from the tip of the antenna with increasing odorant concentration), and their frequency response functions could be fitted by the first-order low-pass filter function used previously to characterize the responses of moth antenna to pheromones (Justus et al. 2005):

$$G(jf) = \beta \cdot \exp(j\angle(2\pi f \Delta u)) \cdot 1/(1 + j2\pi f \nu), \quad (2)$$

where $G(jf)$ is the complex frequency response, β is a constant amplitude, Δu is a pure time delay, and ν is the time constant of the linear filter. The example shown here is for hexyl acetate (Figure 4). This was chosen because it has a relatively short time constant of approximately 12 ms, requiring broadband stimulation for accurate characterization. Equation (2) is shown as the solid lines through the gain and phase data (Figure 4). The true gain units of the frequency response cannot be given because the ratio of odorant molecules to tracer gas is unknown. Here, they are shown as antennal current versus tracer gas concentration (pA/ppm propylene).

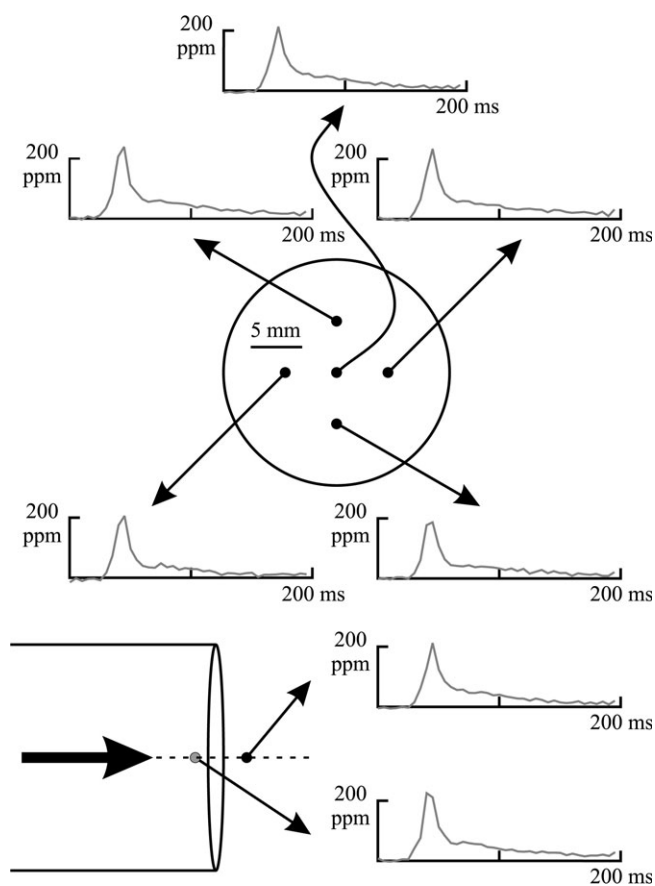


Figure 3 Impulse response functions of tracer gas concentration at varying positions around the experimental animal, estimated using random stimulation (Materials and Methods). The impulse response function represents the theoretical response of the system to an infinitely brief pulse at the input (a pulse of tracer gas in this case). At the end of a normal experiment with the fly in position, the PID probe tip was moved from the normal position (1 mm above the fly head) to positions 5 mm left, right, above, and below (upper traces) and in front of the animal (lower traces). Recordings were made as in Figure 2, but the data were analyzed by the parallel cascade method to estimate the linear impulse response. The peak response occurred at approximately 44 ms in each case, except for the measurement 5 mm in front of the fly, where the value was 42 ms. Drawings of the flow tube mouth are to the scale shown. Lateral positions are all shown relative to an observer at the inlet (fan) end of the flow tube.

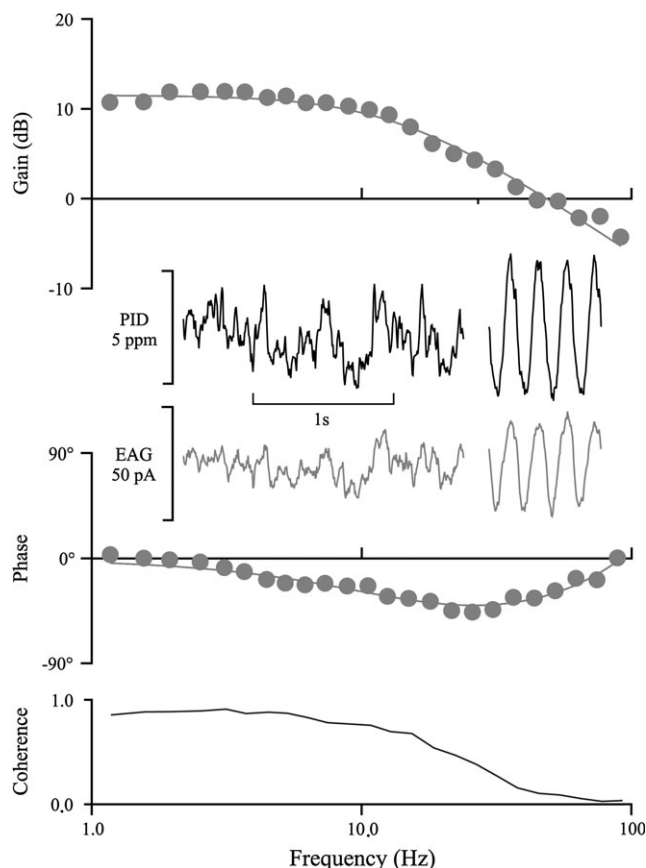


Figure 4 Frequency response function between tracer gas concentration (input) and electroantennogram current (output) for hexyl acetate-stimulated *Drosophila*. See Materials and Methods for odorant delivery details. Gain values, shown in dB, represents the ratio of electroantennogram current from the patch clamp amplifier (10 pA/V) to tracer gas concentration (5.896 ppm/V), so zero dB corresponds to 1.696 pA/ppm. Gain and phase data were fitted by equation (2) (solid lines) with the following parameters: $\beta = 1.94$ pA/ppm, $\nu = 11.85$ ms, $\Delta u = -2.39$ ms. Note that the negative delay due to the PID needle causes the phase relationship to lead at high frequencies, after the initial lag at low frequencies due to the filter function. Inset shows 2 s of original recordings of PID output of tracer gas concentration (upper) and the resulting *Drosophila* electroantennogram current (lower, EAG) during pseudorandom stimulation. On the same inset axes are shown PID and electroantennogram traces obtained during a separate experiment using sinusoidal stimulation with isoamyl acetate.

Experiments were conducted on a total of 42 different animals, and each animal was stimulated with all 4 odorants, in turn, using a random number sequence to create a different order of stimulation for each animal. Total stimulation time for each odor was 100 s. Between different odors, animals received 100 s of airflow without odor. Olfactory frequency response functions were reliable. They were well fitted by equation (2) and had higher coherence function values, with greater bandwidth than the data obtained previously using a turbulent flow system (Justus et al. 2005).

Discussion

Satisfying the initial design criteria

The results may be summarized as follows: 1) Figure 2 shows that tracer gas concentration at the animal was accurately controlled by the input stimulus waveform over a wide frequency range. 2) Figure 3 shows that tracer gas concentration as a function of time was identical except for flow delay in the flow direction within at least 5 mm of the animal in any direction, so flow around the animal was presumably laminar. 3) Figure 4 shows that gas concentration at the animal was linearly related to antennal response, so odorant concentration was linearly related to tracer gas concentration. Note that only item (3) is crucially required for accurate measurement of electrophysiological responses, as shown in the characterization of moth electroantennograms by turbulent flow (Justus et al. 2005). However, item (1) provides the experimenter with control over the type of waveform that can be delivered to the animal, and item (2) reassures us that the odorant concentration at the animal is accurately reflected in the PID recording a short distance away.

The design of the odorant stimulation system resulted from a series of earlier design attempts and tests. Several major design features represent compromises between competing criteria. A longer flow tube encourages laminar flow, but the longer time could also allow mixing in the flow direction, spreading the impulse response function in time and reducing the frequency bandwidth. Similarly, faster airflow (higher fan speed) improves the bandwidth but increases frictional drag and risks more turbulent flow. Similar considerations apply for tube diameter and carrier gas flow rate.

The major design criteria were 1) controlled and measured odorant concentration, 2) constant concentration at short distances from the antenna, 3) maximum available stimulation bandwidth. The system described here meets all these criteria.

The relationship between the silicone bead position and the tracer gas concentration was approximately linear and noise free (Figure 2), so a wide range of odorant stimulus waveforms could be delivered to the animal. For example, it might be useful to test the response to the odorant versus time waveform expected from particular behavioral situations, such as approaching a fruit surface at a known speed.

Tracer gas, and presumably odorant, concentration was highly reliable within 5 mm laterally of the animal (Figure 3), indicating that laminar flow occurs at this flow rate. Measurement in front of the animal gave a very similar impulse response but shifted forward in time by exactly the amount expected from the flow rate. This is an important feature because it is usually impossible to measure tracer gas at the exact location of the receptor. We were able to place the PID probe about 1 mm from the antenna, but the distribution of concentration is so even that measurements up to at least 5 mm away should be adequate to accurately characterize the stimulus.

The frequency range obtained here was wider and better distributed than previously reported using turbulent flow to generate wide bandwidth stimuli to moth antennae (Justus et al. 2005). The turbulent system had difficulty creating low-frequency stimulation, whereas the new system can easily operate down to 0 Hz, with controlled steady concentrations, as shown for the long-pulse stimuli in Figure 2. It also provides a better range of high-frequency stimulation, approaching 100 Hz under the conditions described here, which is about twice the maximum frequency available from the turbulent system. The coherence function was higher than seen in moth antennae, which is notable because of the large size and low-noise recording available from amputated antennae of moths compared with intact *Drosophila*. The frequency responses obtained here were usually consistent up to 100 Hz, but the drop in coherence (Figure 4) indicates that response drops below the noise level before 100 Hz. Preliminary experiments showed that bandwidth can be significantly extended using higher fan speeds, but this was not required for *Drosophila* electroantennograms and may increase concentration gradients as well as reducing mean odorant level.

The wide frequency range was obtained at the cost of relatively high air velocity (2.37 m/s). This presented no problems for *Drosophila* recordings but could conceivably limit usefulness in more delicate preparations. Velocity could be reduced for preparations with slower responses than *Drosophila*, or technical improvement may allow lower velocities in the future.

Drosophila electroantennograms

Discussion of the dynamic properties of *Drosophila* electroantennograms to different odorants is beyond the scope of this article, but we note the general similarity of the low-pass response characteristics (Figure 4) to the pheromone responses in 2 moth species, with an even shorter time constant in *Drosophila* than the fastest response of *Spodoptera exigua* (Justus et al. 2005). This suggests that rapid response to odorants is behaviorally important in *Drosophila*. A noticeable difference from the moth data is the lack of any delay in the antennal responses. The negative time delay of about -2.5 ms seen here corresponds closely to the estimated delay

in the PID probe, so the antenna actually detects the odorant before the tracer gas has passed along the probe needle. The delay of 5–10 ms in moth electroantennograms was tentatively assigned to action potential conduction along the antenna, which would be much faster in the tiny *Drosophila* antenna.

Summary

The stimulation system described here promises to be an important new tool for studying the dynamic responses of olfactory receptor organs, providing a controlled signal similar to those already available for dynamic stimulation of mechanoreceptors and photoreceptors. The system is not limited to electroantennograms, or to *Drosophila*, but should be useful for other measurements, such as single-unit recording, as well as for other small animals.

Acknowledgements

We thank Päivi H. Torkkeli for comments and suggestions on the article. Julia Schuckel gave technical support. Support for this work was provided by the Canadian Institutes of Health Research.

References

- Alcorta E. 1991. Characterization of the electroantennogram in *Drosophila melanogaster* and its use for identifying olfactory capture and transduction mutants. *J Neurophysiol.* 65:702–714.
- Bau J, Justus KA, Loudon C, Cardé RT. 2005. Electroantennographic resolution of pulsed pheromone plumes in two species of moths with bipectinate antennae. *Chem Senses.* 30:771–780.
- Bendat JS, Piersol AG. 1980. Engineering applications of correlation and spectral analysis. New York: John Wiley & Sons.
- Cooley JW, Tukey JW. 1965. An algorithm for the machine calculation of complex Fourier series. *Math Comput.* 19:297–301.
- Dobritsa AA, van der Goes van Naters, Warr CG, Steinbrecht RA, Carlson JR. 2003. Integrating the molecular and cellular basis of odor coding in the *Drosophila* antenna. *Neuron.* 37:827–841.
- French AS, Holden AV, Stein RB. 1972. The estimation of the frequency response function of a mechanoreceptor. *Kybernetik.* 11:15–23.
- French AS, Kuster JE. 1981. Sensory transduction in an insect mechanoreceptor: extended bandwidth measurements and sensitivity to stimulus strength. *Biol Cybern.* 42:87–94.
- French AS, Marmarelis VZ. 1999. Nonlinear analysis of neuronal systems. In: Windhorst U, Johansson H, editors. Modern techniques in neuroscience research. Berlin (Germany): Springer. p. 627–640.
- French AS, Wong RKS. 1977. Nonlinear analysis of sensory transduction in an insect mechanoreceptor. *Biol Cybern.* 26:231–240.
- Fuortes MGF, Hodgkin AL. 1964. Changes in time scale and sensitivity in the ommatidia of *Limulus*. *J Physiol.* 172:239–263.
- Hazel MH, Ianowski JP, Christensen RJ, Maddrell SH, O'Donnell MJ. 2003. Amino acids modulate ion transport and fluid secretion by insect Malpighian tubules. *J Exp Biol.* 206:79–91.
- Justus KA, Cardé RT, French AS. 2005. Dynamic properties of antennal responses to pheromone in two moth species. *J Neurophysiol.* 93:2233–2239.
- Marmarelis PZ, Marmarelis VZ. 1978. Analysis of physiological systems: the white-noise approach. New York: Plenum Press.
- Marmarelis PZ, Naka KI. 1973. Nonlinear analysis and synthesis of receptive field responses in catfish retina I horizontal cells to ganglion cell chain. *J Neurophysiol.* 36:605–618.
- Pringle JW, Wilson VJ. 1959. The response of a sense organ to a harmonic stimulus. *J Exp Biol.* 29:220–234.
- Stensmyr MC, Giordano E, Balloi A, Angioy AM, Hansson BS. 2003. Novel natural ligands for *Drosophila* olfactory receptor neurones. *J Exp Biol.* 206:715–724.
- Vetter RS, Sage AE, Justus KA, Cardé RT, Galizia CG. 2006. Temporal integrity of an airborne odor stimulus is greatly affected by physical aspects of the odor delivery system. *Chem Senses.* 31:359–369.
- Vickers NJ, Christensen TA, Baker TC, Hildebrand JG. 2001. Odour-plume dynamics influence the brain's olfactory code. *Nature.* 410:466–470.
- Vosshall LB, Amrein H, Morozov PS, Rzhetsky A, Axel R. 1999. A spatial map of olfactory receptor expression in the *Drosophila* antenna. *Cell.* 96:725–736.
- Widmer A, Panek I, Höger U, Meisner S, French AS, Torkkeli PH. 2006. Acetylcholine receptors in spider peripheral mechanosensilla. *J Comp Physiol A Neuroethol Sens Neural Behav Physiol.* 192:85–95.
- Yao CA, Ignell R, Carlson JR. 2005. Chemosensory coding by neurons in the coeloconic sensilla of the *Drosophila* antenna. *J Neurosci.* 25:8359–8367.

Accepted April 16, 2007